Photoacoustic correlation spectroscopy and its application to low-speed flow measurement

Sung-Liang Chen,[1] Tao Ling,[1] Sheng-Wen Huang,[2] Hyoung Won Baac,[1] and L. Jay Guo[1,*]

[1]*Department of Electrical Engineering and Computer Science, University of Michigan, Ann Arbor, Michigan 48109, USA*

[2]*Department of Bioengineering, University of Washington, Seattle, Washington 98195, USA*

**Corresponding author: guo@umich.edu*

Received January 5, 2010; accepted February 25, 2010;
posted March 9, 2010 (Doc. ID 122138); published April 14, 2010

A photoacoustic correlation technique, inspired by its optical counterpart—the fluorescence correlation spectroscopy (FCS)—was tested for the first time, to our knowledge, to demonstrate the feasibility of low-speed flow measurement based on photoacoustic signal detection. A pulsed laser was used to probe the flow of light-absorbing beads. A photoacoustic correlation system of 0.8 s temporal resolution was built and flow speeds ranging from 249 to 14.9 μm/s with corresponding flow times from 4.42 to 74.1 s were measured. The experiment serves as a proof of concept for photoacoustic correlation spectroscopy, which may have many potential applications similar to the FCS.

OCIS codes: 120.7250, 170.5120.

Fluorescence correlation spectroscopy (FCS) is a powerful technique widely used in analytical chemistry and biological research [1]. In the FCS, the fluctuation of fluorescence intensity of a small number of fluorescent molecules is analyzed using temporal correlation. The FCS has found a wide range of applications [2,3]. We propose a technology, photoacoustic correlation spectroscopy (PACS), by extending the fluorescence detection in the FCS to the acoustic signal domain. PACS is based on pulsed laser excitation. Autocorrelation is performed using measured photoacoustic (PA) signals, and the term "spectroscopy" refers to the time-spectrum rather than the common usage as a frequency spectrum. PACS is different from other techniques using PA effects in correlation measurements, such as photoacoustic spectroscopy (PAS) [4] and correlation photoacoustic spectroscopy (CPAS) [5]. PAS was to analyze the absorbing chemical groups of samples from the measured infrared spectrum. CPAS measures the cross correlation between the excitation source and the detected acoustic response. CPAS was mainly used to study static properties such as depth-profiling and thermal imaging. In contrast, the specific purpose of the PACS technique is to study functional dynamics of PA species.

PACS could open up a range of applications in medical diagnosis. As one example, the analysis of microcirculation system provides a unique comprehension of disease processes [6]. Current methods include Doppler-related techniques and histological sectioning. However, these techniques in studying microcirculation have been restricted by issues of invasiveness, low resolution, limited imaging depth, and minimum measurable flow speed [7]. Take Doppler techniques, for example. The Doppler ultrasound method is not easy to detect flow speeds less than 1 mm/s [8]. Doppler optical coherence tomography has difficulties in flow measurement at depths greater than 1 mm [9]. One way to overcome these limitations is using PA signals from the red blood cells (RBCs) excited by a pulsed laser, which circumvents the diffusive light scattering in tissues [10].

In this Letter, we conduct experiments on flow measurement to demonstrate the feasibility of the PACS technique. The PACS flowmetry for the assessment of a microvascular blood flow has several advantages. (1) It provides a label-free measurement because of the high optical contrast between RBCs and the surrounding tissues [11]. (2) Low scattering of sound signals enables a high imaging depth. (3) Wide range flow speeds can be measured by properly designed temporal resolution and probe beam size. (4) A PA microscopy scheme can be used to provide a high spatial resolution [12].

Light-absorbing beads generate PA waves when they absorb laser energy and undergo an instantaneous thermal expansion. In the PACS, we name the counterpart of the fluorescence intensity in the FCS as the PACS strength. It can be expressed as

$$P(t) \equiv \int I(r)n(r,t)d^3r, \tag{1}$$

where $I(r)$ is the normalized spatial fluence distribution of the laser beam and $n(r,t)$ is the bead concentration at position r and time t. The laser beam used in our PACS setup defines the probe volume. When the beads move in and out of the volume, the number of beads present in this volume, denoted as $n_{\text{in}}(t)$, fluctuates. Because the PA pressure amplitude is not directly proportional to the PACS strength $P(t)$, the information of $P(t)$ needs to be extracted by proper signal processing from the measured PA signals. In our flow-measurement configuration, a one-dimensional step excitation profile was used. Thus, $I(x)=1$ at $|x|\leq w/2$ and $I(x)=0$, otherwise, where w is a width of the probe laser beam. The temporal autocorrelation of $P(t)$ provides information about the average duration and strength of the fluctuations [13]. Specifically, the decay profile of the autocorrelation function $G(\tau)$ reveals the beads' dwell time in the

probe volume. The magnitude of $G(0)$ is related to the number density of the beads in the probe region. The normalized autocorrelation function can be calculated as

$$G(\tau) = \langle \delta P(t)\, \delta P(t+\tau)\rangle / \langle P(t)\rangle^2, \qquad (2)$$

where $\delta P(t) = P(t) - \langle P(t)\rangle$ is the fluctuation of $P(t)$ and $\langle\ \rangle$ denotes an ensemble average.

We choose a flow experiment because it is easy to obtain a range of dwell times. The analysis of flow for a step laser profile has been studied [14]. With a flow speed V of the beads, the autocorrelation function takes the following form:

$$G(\tau)/G(0) = \begin{cases} 1 - \tau/\tau_0, & \text{for } \tau \le \tau_0 \\ 0, & \text{for } \tau > \tau_0 \end{cases}, \qquad (3)$$

where $t_0 = w/V$. Here, the diffusion of the beads owing to the Brownian motion is neglected, which is a reasonable assumption considering the long diffusion time, $(w^2/16)(6\pi\eta a/k_B T) \approx 8\times 10^6$ s [15,16], where the Boltzmann constant is $k_B = 1.38\times 10^{-23}$ J/K, the temperature is $T = 300$ K, the viscosity coefficient is $\eta = 10^{-3}$ Pa s, the bead radius is $a = 24.5$ μm, and the probe beam size is $w = 1.1$ mm.

The experimental setup is shown in Fig. 1. A 532 nm pulsed laser (Surelite I-20, Continuum, Santa Clara, Calif.) generating 6 ns pulses with a 20 Hz repetition rate was used as the probing light source. The laser beam (fluence of ~ 70 mJ/cm^2) illuminated the flow sample [49 μm diameter black polystyrene (PS) beads in water] with a beam width of 1.1 mm. A microring resonator was used to detect the PA signals [17,18]. Assuming that the probe volume is around the origin, the detector was positioned in the x–z plane, $(x, 0, z)$, as shown in Fig. 1. The photodetector output was fed to an oscilloscope (WaveSurfer 432, LeCroy, Chestnut Ridge, NY). Beads were flowing in a tubing (inner diameter of 0.8 mm) driven by a syringe pump. Flow rates were calibrated from 200 to 14 μm/s using a microscope.

Figures 2(a)–2(c) show the measured PA signals from the PS beads at a calibrated flow speed of 33 μm/s. Figures 2(a) and 2(b) show the temporal PA waveform taken at a particular elapsed time before and after applying a low-pass filter (cutoff frequency

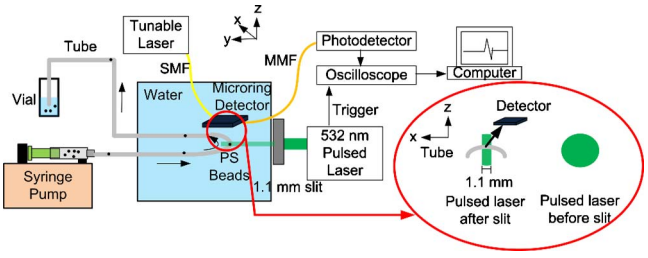

Fig. 1. (Color online) Experimental setup for PACS flow measurement: SMF, MMF, and PS stand for single-mode fiber, multi-mode fiber, and polystyrene beads, respectively. Beads flow in the x-direction. The PA signals were detected by using a microring resonator positioned in the x-z plane. The shape of the pulsed laser before and after a slit is illustrated.

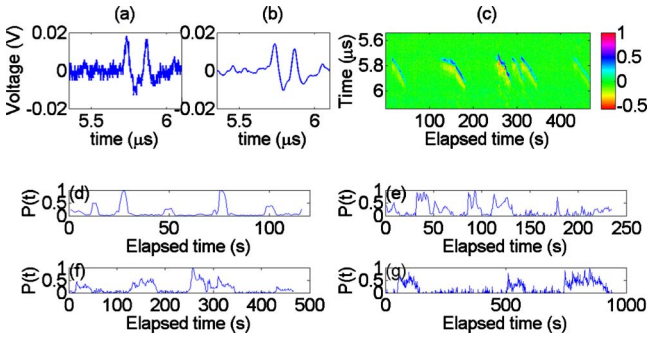

Fig. 2. (Color online) (a) Detected raw PA signals at a calibrated flow speed of 33 μm/s and at elapsed time = 309.1 s. (b) Signals after filtering. (c) Detected PA signals as a function of elapsed time, measured at the calibrated speed of 33 μm/s. The average distance from the beads to the detector was ~ 8.5 mm. (d)–(g) PACS strength fluctuation as a function of elapsed time. PACS strengths in (d), (e), (f), and (g) correspond to calibrated speeds of 200, 90, 33, and 14 μm/s, respectively.

of 50 MHz). The complete PA signals collected are shown in Fig. 2(c). As time elapses, the temporal PA signals appear from 5.75 to 5.95 μs. Thus, we can determine that the one-dimensional flow direction is away from the detector. For measuring three-dimensional flow vectors, the line scan FCS [19] can be applied to the PACS. Figures 2(d)–2(g) show the PACS strength $P(t)$ for four calibrated speeds. It was extracted using the collected temporal PA data to within a constant scaling factor by taking the rms value of the measured PA signals, which is suitable for a low-concentration solution. Owing to a finite duration needed for each data transmission from the oscilloscope to a computer, the available temporal resolution of our current PACS system is 0.8 s, meaning one sample of $P(t)$ per 0.8 s. Noise in $P(t)$ estimate was offset to zero for more accurate estimation of $G(0)$ [15]. Figures 2(d)–2(g) show that the bead dwell time becomes longer as the speed decreases. Different noise levels in $P(t)$ are due to different devices' sensitivities. The signal-to-noise ratios of the filtered PA signals in the four cases were estimated as 35, 26, 29, and 22 dB.

The PACS curves are shown in Fig. 3(a). The dotted points are autocorrelation curves calculated from Eq. (2). The solid curves are the fits using Eq. (3). The dwell times τ_0 obtained from PACS curves were 4.42 -74.1 s. The measured flow speeds calculated from the relation $V = w/\tau_0$ were 249–14.9 μm/s. In Fig. 3(b), the dotted points are the speeds by the PACS measurement and the solid line represents results from direct measurement, which shows excellent agreement between the two. The discrepancy in the case of the faster flow speed might be owing to limited fitting points.

The extracted average bead number $\langle n_{\text{in}}\rangle$ was 0.53. Accordingly, the concentration can be estimated as 0.96 mm^{-3} $[=0.53/(1.1\pi(0.8/2)^2)]$, which is a little different from the designed concentration of ~ 0.69 mm^{-3}. The former could have been overestimated because the nonuniform spatial fluence distribution of laser can result in a less-than-1 volume con-

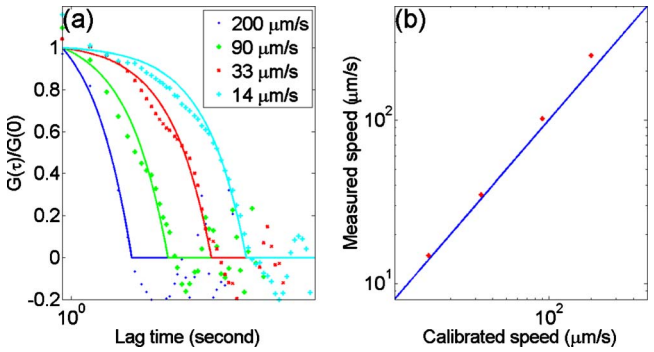

Fig. 3. (Color online) (a) PACS curves of designed flow speeds of 200, 90, 33, and 14 μm/s. The solid curves are the corresponding fits. (b) The measured flow speeds by the PACS technique, shown in stars, versus the calibrated flow speeds. The solid line represents the results from direct measurement.

trast [15,20] and thus an underestimated probe volume. Longer measurement time and lower noise are helpful to determine the concentration more accurately. To measure a higher concentration in PACS, either a better detection scheme to distinguish $n_{\mathrm{in}}(t) \gg 1$ or a small probe volume can be used. In the former case, a detector array enables imaging capability. In the latter case, the temporal resolution of a PACS system should also be improved according to the relation $t_0 = w/V$. Otherwise, the maximum measurable flow speeds would be limited. As V increases, the flow time τ_0 decreases and eventually approaches the limit of the system's temporal resolution. A small probe volume also expands the minimum measurable V, which has no theoretical limitation in the PACS flowmetry, by preventing prohibitively long time for measurement. Combining the two methods, PACS techniques can be further engineered for clinical applications.

To show the potential of PACS to study microcirculation at significant depths, we analyze a case of PA detection of an RBC. Assuming that the effective noise-equivalent pressure of a microring detector array is 2 Pa over 1–80 MHz and a 7 μm RBC, the imaging depth is estimated as 4.6 mm by using an analysis similar to that in [17] with the following parameters: $\mu_{\mathrm{eff}}^{\mathrm{blood}} = 50\ \mathrm{cm}^{-1}$, $\mu_{\mathrm{eff}}^{\mathrm{tissue}} = 1\ \mathrm{cm}^{-1}$, $J_0 = 20\ \mathrm{mJ/cm}^2$, and $A = 20\ \mathrm{dB/cm}$. In comparison, the FCS for blood flow is limited by the optical transport mean free path, ~1 mm in the human skin. The spatial resolution of the probe volume can be several micrometers [12]. So it is feasible to use the PACS technique to study randomly oriented networks of small microvessels. Our analysis shows that PACS has a potential to study microcirculation with a low flow speed in small capillaries. The high sensitivity and wideband properties of the microring detector [17,18] enable deep imaging depths and high spatial resolutions.

In summary, a PA correlation technique for low-speed flow measurement has been developed. We have demonstrated that the PACS technique can accurately measure bead flow speeds as slow as 14.9 μm/s. The technique has abilities to discriminate flow direction and to measure the concentration of solution. Exploring PACS for other applications will be a valuable future work.

We would like to thank Dr. Yu-Chung Chang for useful discussion on FCS. Support from the National Institutes of Health (NIH), grant EB007619-01A1, is gratefully acknowledged.

References

1. E. L. Elson, J. Biomed. Opt. **9**, 857 (2004).
2. S. T. Hess, A. A. Heikal, and W. W. Webb, Biochemistry **41**, 697 (2002).
3. S. A. Kim, K. G. Heinze, M. N. Waxham, and P. Schwille, Proc. Natl. Acad. Sci. USA **101**, 105 (2004).
4. J. Irudayaraj and H. Yang, J. Food. Eng. **55**, 25 (2002).
5. S. A. Telenkov and A. Mandelis, J. Biomed. Opt. **11**, 044006 (2006).
6. B. Fagrell and M. Intaglietta, J. Intern Med. **241**, 349 (1997).
7. D. E. Goertz, D. A. Christopher, J. L. Yu, R. S. Kerbel, P. N. Burns, and F. S. Foster, Ultrasound Med. Biol. **26**, 63 (2000).
8. D. A. Christopher, P. N. Burns, J. Armstrong, and F. S. Foster, Ultrasound Med. Biol. **22**, 1191 (1996).
9. J. Moger, S. J. Matcher, C. P. Winlove, and A. Shore, J. Phys. D **38**, 2597 (2005).
10. H. Fang, K. Maslov, and L. V. Wang, Phys. Rev. Lett. **99**, 184501 (2007).
11. R. G. M. Kolkman, E. Hondebrink, W. Steenbergen, and F. F. M. de Mul, IEEE J. Sel. Top. Quantum Electron. **9**, 343 (2003).
12. K. Maslov, H. F. Zhang, S. Hu, and L. V. Wang, Opt. Lett. **33**, 929 (2008).
13. E. Haustein and P. Schwille, Curr. Opin. Struct. Biol. **14**, 531 (2004).
14. H. Asai, Jpn. J. Appl. Phys. **19**, 2279 (1980).
15. Y.-C. Chang, J. Y. Ye, T. Thomas, Y. Chen, J. R. Baker, and T. B. Norris, Opt. Express **16**, 12640 (2008).
16. D. Vobornik, D. S. Banks, Z. Lu, C. Fradin, R. Taylor, and L. J. Johnston, Appl. Phys. Lett. **93**, 163904 (2008).
17. S.-W. Huang, S.-L. Chen, T. Ling, A. Maxwell, M. O'Donnell, L. J. Guo, and S. Ashkenazi, Appl. Phys. Lett. **92**, 193509 (2008).
18. S.-L. Chen, S.-W. Huang, T. Ling, S. Ashkenazi, and L. J. Guo, IEEE Trans. Ultrason. Ferroelectr. Freq. Control **56**, 2482 (2009).
19. X. Pan, X. Shi, V. Korzh, H. Yu, and T. Wohland, J. Biomed. Opt. **14**, 024049 (2009).
20. J. Mertz, C. Xu, and W. W. Webb, Opt. Lett. **20**, 2532 (1995).